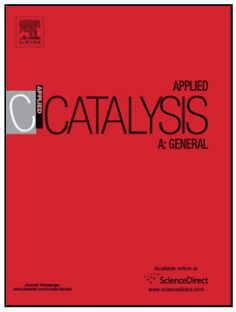

Title: Effect of the preparation method of supported Au nanoparticles in the liquid phase oxidation of glycerol

Author: Nikolaos Dimitratos Alberto Villa Laura Prati Ceri Hammond Carine E. Chan-Thaw James Cookson Peter T. Bishop

PII: S0926-860X(15)30307-0
DOI: http://dx.doi.org/doi:10.1016/j.apcata.2015.12.031
Reference: APCATA 15705

To appear in: *Applied Catalysis A: General*

Received date: 3-11-2015
Revised date: 21-12-2015
Accepted date: 23-12-2015

Please cite this article as: Nikolaos Dimitratos, Alberto Villa, Laura Prati, Ceri Hammond, Carine E.Chan-Thaw, James Cookson, Peter T.Bishop, Effect of the preparation method of supported Au nanoparticles in the liquid phase oxidation of glycerol, Applied Catalysis A, General http://dx.doi.org/10.1016/j.apcata.2015.12.031

Effect of the preparation method of supported Au nanoparticles in the liquid phase oxidation of glycerol

Running title: Effect of polymer, concentration, metal and heat treatment in the synthesis of Au catalysts and catalytic activity in the liquid phase oxidation of glycerol.

Nikolaos Dimitratos[a,b*] sacnd1@cardiff.ac.uk, Alberto Villa[d**] Alberto.Villa@unimi.it, Laura Prati[d], Ceri Hammond [a,b], Carine E. Chan-Thaw[d], James Cookson[c], Peter T. Bishop[c]

[a]Cardiff Catalysis Institute, School of Chemistry, Cardiff University, Main Building, Park Place, Cardiff, CF103AT,UK

[b]UK Catalysis Hub, Research Complex at Harwell (RCaH), Rutherford Appleton Laboratory, Harwell, Oxon, OX11 0FA, UK

[c]Johnson Matthey Technology Centre, Blount's Court, Sonning Common, Reading, RG4 9NH, UK

[d]Dipartimento di Chimica, Università degli Studi di Milano, via Golgi 19, Milano, 20133, Italy

[*]Corresponding author at: Cardiff Catalysis Institute, School of Chemistry, Cardiff University, Main Building, Park Place, Cardiff, CF103AT, UK, UK Catalysis Hub, Research Complex at Harwell (RCaH), Rutherford Appleton, Laboratory, Harwell, Oxon, OX11 0FA, UK, Tel.: +44(0)2920874082

[**]Corresponding author at: Dipartimento di Chimica, Università degli Studi di Milano, via Golgi 19, Milano, 20133, Italy, Tel.: +39 02 503 14361, Fax +39 02 503 14405.

Graphical Abstract

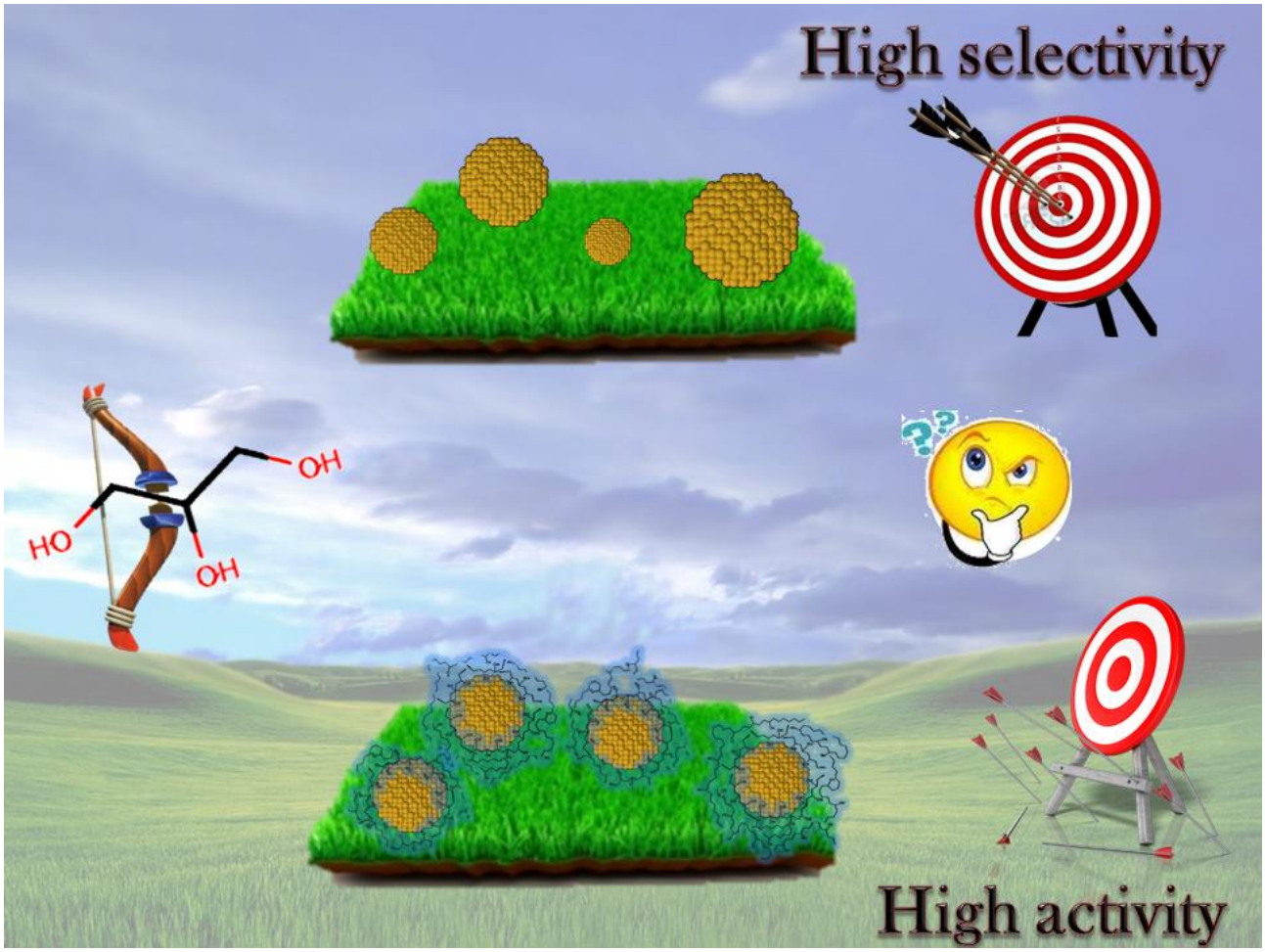

Highlights

- Au nanoparticles (NPs) were prepared and supported on AC and TiO_2.
- The effect of Au concentration and the influence of the stabilizer were studied.
- The stabilizer amount and Au concentration produced Au NPs with different size.
- The catalytic performance of the Au catalysts was studied for glycerol oxidation.
- Activity and selectivity were ruled out by gold size and stabilizer amount.

Abstract

Catalytically-active gold nanoparticles that are stable in aqueous solution have been prepared by sodium borohydride reduction of the respective metal salts in the presence of the stabilising polymer PVA (polyvinylalcohol). By controlling the ratio of the polymer to the metal, nanoparticles with different particle size and size distribution were synthesised. By varying the concentration of the gold and PVA/Au wt/wt ratio, well-defined nanoparticles with mean diameters from 3 to 5 nm could be fabricated. In general increasing the concentration of Au precursor, bigger particles size were obtained. Furthermore decreasing the amount of PVA, bigger particles were obtained, with the exception of the catalysts synthesized in presence of a large amount of PVA (PVA/Au =2) wt/wt. Probably, in presence of an excess of protective agent, the immobilization of the Au nanoparticles onto the support is more difficult, leading to partial aggregation and coalescence of Au. In addition, the studies on the effect of heat pre-treatment revealed a higher resistance to aggregation of Au nanoparticles supported on titania than on activated carbon. A selected series of the synthesised supported materials were studied in the liquid phase oxidation of glycerol with the purpose of correlating catalytic activity and selectivity with particle size and metal choice. We demonstrated that by both particles size and amount of protective agent strongly influence the activity and selectivity.

Keywords: gold; nanoparticles; liquid phase oxidation; heat treatment; stabiliser effect

1. Introduction

Nanoparticles of gold have attracted significant attention in recent years due to their unique properties and their potential in a wide range of applications in the fields of microelectronics [1,2], sensing [3] non-linear optical materials [4] and catalysis [5,6]. For example, in the field of catalysis (both homogeneous and heterogeneous) exciting progress is being made using gold, as demonstrated by recent reviews [7-10]. This is particularly prominent since gold has long believed to be catalytically inactive and not worthy of study. In fact, gold-based catalytic systems have recently been shown to be active and selective in numerous organic transformations, such as the catalytic oxidation of carbon oxide [11-16], hydrochlorination of ethyne [17], propene epoxidation [18], the oxidation of carbohydrates, polyols and alcohols [19-33] and the synthesis of hydrogen peroxide [34-39]. In particular, polyvinyl alcohol (PVA) has been widely used for preparing gold based catalyst for liquid phase reaction, providing good metal dispersion regardless of the chosen support, and increasing the durability of the catalyst [40]. Recent papers report the role of the capping agent in the catalytic activity, in particular in mediating the interaction between the reactant and the active sites (on the metal and/or on the support) [41, 42].

In the present study, we investigated the effect on the metal particle size and its particle size distribution by varying the initial Au precursor concentration and the weight ratio of stabilising polymer to the metal (PVA/Au). Moreover, our aim was to deposit the preformed nanoparticles onto different support materials (namely activated carbon and titania) and examine the effect of the support and subsequent heat treatments on the supported nanocatalysts. The characterisation of selected gold colloids and supported gold colloids was investigated by means of transmission electron microscopy (TEM), energy dispersive X-ray (EDX) analysis and X-ray photoelectron spectroscopy (XPS). The synthesised catalysts were tested in the liquid phase selective oxidation of glycerol.

Selective oxidation in the presence of molecular oxygen represents a highly important challenge from an applicative point of view. In fact, the selective oxidation of glycerol is a growing area of research intensity, as it permits the upgrading of an inexpensive waste chemical into more valuable compounds, which is both environmentally and economically beneficial. In the oxidation of glycerol, a variety of products can be formed depending on the reaction conditions. These products could be dihydroxyacetone (DIXA), glyceraldehyde (GLYHYDE), glyceric acid (GLYA), glycolic acid (GLYCA), hydroxypyruvic acid (HPYA), mesoxalic acid (MOXALA), oxalic acid (OXALA) tartronic acid (TARAC) and formic acid (FOA) (Scheme 1). Controlling the selectivity of the reaction to achieve high selectivity to the desired products by choosing the appropriate catalysts and reaction conditions is highly desirable.

2. Experimental

2.1. Materials

$HAuCl_4$ (purity > 99.0%) was obtained from Alfa Aesar, PVA (Mw=13000 –23000, 98% hydrolysed) and $NaBH_4$ was purchased from Aldrich. All of the starting materials were used as supplied, without further purification. Norit Carbon GSX (1292 m^2 g^{-1}) was used as carbon support, the titania support used was anatase (99.7%, , 45 m^2 g^{-1}) and were supplied by Alfa Aesar.

Stock aqueous solutions $HAuCl_4$ ([Au] = 0.199 M), PVA (1% w/w) and $NaBH_4$ (0.1, 0.3M) were prepared. The aqueous solutions of PVA (1 wt%) and $NaBH_4$ (0.1M, 0.3M) were freshly prepared prior to each experiment. Glycerol (88% wt solution), glyceric acid and all intermediate products were acquired from Fluka. Deionised water (Milli-Q purified) was used in all the experiments. Gaseous oxygen was obtained from SIAD at a 99.99% purity.

2.2. Synthesis of supported Au nanoparticles

To an aqueous solution of $HAuCl_4$ the relevant amount of PVA solution was added under vigorous stirring. The resulting yellow solution was then stirred for 3 minutes at room temperature. The subsequent rapid addition of an aqueous solution of $NaBH_4$, (0.1 M, $NaBH_4$/Au (mol/mol) = 5) resulted in the chemical reduction of the metal. The colour of the solution changed immediately from light yellow to red, indicating the formation of gold sol [43]. The solution was then left under stirring for one hour. The formed nanoparticles were then added to the desired amount of the support in order to produce a 1wt% loaded catalyst. The solution was acidified to pH 1 via the addition of sulfuric acid in order to assist deposition onto the support. The stirring of the slurry was maintained for 1 hour. This time was sufficient for total adsorption of the Au sol on the support, which was indicated by decolouration of the solution. After 2 hours, the slurry was filtered and the filtrate was colourless. The catalyst was then washed thoroughly with distilled water (neutral mother liquors) and dried at 80 °C under vacuum for 24 hours.

The synthesis of Au nanoparticles with different gold concentration was performed by altering the volume of the Au aqueous solution (from 200 ml to 2.5 L), whilst keeping the gold concentration fixed. The following concentrations were chosen for examination: [Au] = ($1.02*10^{-3}$, $5.08*10^{-4}$ and $1.69*10^{-4}$ M), Table 1.

In the case of synthesising Au colloids with different PVA/Au wt/wt ratio, the following PVA/Au ratios were chosen: (0.3, 0.65, 1.2 and 2.0), Table 1.

Finally, the influence of heat pre-treatment was studied on the different supports (Carbon, titania) by calcining samples at 250 ºC at static air conditions using a heating rate of 5 °C /min and cooling at a rate of 30 °C/min.

2.3. Characterisation

For the morphological characterisation of the supported and unsupported gold particles, transmission electron microscopy (TEM) was carried out on an FEI tecnai F20 TEM operating at 200 kV and Energy Dispersive X-ray analysis (EDX) was carried out using an EDAX r-TEM with a 30 mm^2 Si(Li) detector. To obtain suitable samples for TEM characterisation, the samples were treated as follows: A drop of the colloidal solution was placed on a carbon film on a copper TEM grid and was allowed to dry by slow evaporation. For the supported gold samples, the samples were crushed and then dusted onto a holey carbon film on a copper TEM grid such that the sample remained in the native form. Particle sizes and particle size distributions were determined from the TEM micrographs by measuring the sizes of a large number of individual particles (typically between 100 and 800 particles) using digital micrograph (supplied by Gatan). The gold content of the samples including possible contamination of chloride, sodium, or sulphur ions was determined by energy-dispersive X-ray analysis (EDX), which was performed on a Leica S-440i, tungsten filament scanning electron microscope equipped with an Oxford Instruments EDX system. The size distribution can be fitted by a log-normal function. ICP was used to determine the weight percentage of the metal loaded on the support after the immobilisation step. Samples for analysis were prepared by dissolving 0.1 g of the dried sample in a solution of aqua regia, followed by the addition of 250 ml milli-Q water for diluting the sample. ICP analyses of selected samples (Au/C and Au/TiO_2) verified that the loading of Au was 1 wt% for all the catalysts.

For selected colloidal solutions, UV-vis spectra were recorded on a UV-vis- spectrometer in mili-Q water between 200-900 nm using a quartz cuvette.

For selected samples XPS analyses were performed using a Thermo V.G. Scientific ESCALAB 250. Powders of the supported nanoparticles were dusted onto a conductive carbon tape and thereby mounted on a sample stub. The exciting radiation used in the studies was monochromised aluminium Ka radiation in a 650μm spot at 200 W power. The energy reference used was (i) elemental carbon at 284.55 eV for Au/C samples and (ii) of poly(vinyl alcohol at 284.85 eV for Au/TiO_2 samples. XPS analyses showed the presence of Au in the metallic state (Au $4f_{7/2}$ 83.1-84.1 eV) on dried and calcined samples (see supplementary information, Table S1, Figures S1 and S2), whereas low amounts of Chlorine and sulphur (<0.5%) were detected on the surface.

2.4. Oxidation reactions

The oxidation of glycerol was carried out in a stirred reactor (100 ml, Parr Autoclave reactor). The vessel was charged with basic glycerol solution (0.3 M and NaOH / Glycerol ratio = 4, mol/mol) and the desired amount of catalyst was suspended in the solution. The autoclave was then

purged 5 times with oxygen, leaving the vessel at 3-bar gauge. The reaction mixture was raised to the required temperature and the stirrer set at 1500 rpm. Samples from the reactor were taken periodically, *via* a sampling system, ensuring that the volume purged before sampling was higher than the tube volume. Phosphoric acid (0.1wt% solution) was used as the eluent.

For the identification of the products a comparison with the original samples was run and analysis of the products performed by using a high-performance chromatography (HPLC) with UV and refractive index (RI) detection (column, Alltech OA-10308, 300mm × 7.8mm).

For the quantification of the reactant-products the external calibration method was used. The activities of catalysts were reported based on turnover frequency (moles of glycerol converted per mole of surface atoms per hour), calculated based on the total metal loading. Calculations of the number of exposed surface atoms were performed by assuming that all the nanoparticles had cub-octahedral morphology with cubic close-packed structure.

3. Results and discussion

3.1. Fivefold scaling-up of colloidal preparation

The preparation of colloidal solutions were initially undertaken using 10 mg of Au metal and with a gold concentration of [Au] = $5.08*10^{-4}$ M with PVA/Au= 0.65. Scaling up of this preparation method was performed by increasing the Au amount (from 10 to 50 mg) and the volume of milli-Q water in order to maintain constant the Au concentration ([Au] = $5.08*10^{-4}$ M). Analysis of the colloidal solutions using TEM revealed that the mean particle size and particle size distribution (Figure 1) were in a similar range for both colloidal solutions (3.2 nm for the former colloid and 3.5 nm for the latter). In the last case, particle distribution analysis evidenced a higher percentage of particles in the range of 6-14 nm. During the synthesis, the same stirrer speed was used in order to minimise the difference in the agitation of the solutions during the reduction process. It is evident from the results that similar Au particles were obtained when the scaling-up of the process was performed. Moreover, ICP analyses of selected samples verify that the loading of Au was 1wt%, whereas XPS analyses showed the presence of Au in the metallic state on dried and calcined samples. These results encouraged us to continue the synthesis of Au colloids at this scale (50 mg of Au).

3.2. Effect of Au concentration and PVA/Au wt/wt ratio on the 1 wt% Au/C samples

A number of parameters can influence the resulting particle size and morphology of Au colloids, such as concentration of Au precursor and PVA/Au wt/wt ratio. This study was thus

performed in order to determine the effect of the Au concentration and the polymer to gold ratio on the size of the gold supported nanoparticles. The Au concentration was varied between 10^{-3} and 10^{-4} M. In Table 1 the median particle size of the 1 wt% Au/C and Au/TiO_2 samples are reported, whereas TEM images and particles distribution of all the samples are presented in Figure 2, (Figures S3-S6). In general, by decreasing the Au concentration (compared at the same PVA/Au wt/wt ratio), a decrease in the mean particle size was observed (Table 1). However, it is evident that the mean gold particle size depends not only on the concentration of the Au sol, but also on the PVA/Au ratio.

At the highest Au concentration used ($1.02*10^{-3}$ M) and by increasing the PVA/Au wt/wt ratio from 0.3 to 1.2, the average particle diameter was not affected significantly and it was observed in the range of 4.7 to 5.1 nm (Table 1). Surprisingly, further increase of PVA/Au wt/wt ratio produced larger nanoparticles with average gold particle diameter of 5.8 nm. A similar result has been observed using Poly(diallyldimethylammonium) chloride (PDDA) as protective agent at agent/Au ratios higher than 1.2 [19]. It has been observed that with excess of protective agent, the immobilization of the Au nanoparticles onto the support is more difficult, leading to partial aggregation and coalescence of Au as evidenced by the presence of bigger particles in the range of 8-22 nm (Figure 2d). The catalysts with PVA/Au=2 represents an exception to the trend observed for the others PVA/Au ratios regardless Au concentration and supported used. Moreover, a broader diameter distribution was observed as the PVA to gold ratio decreased (Figure 2). In fact, by analysing different areas of the samples synthesised with PVA/Au = 0.3 wt/wt, it was found that some of the gold particles were agglomerated in a few large particles; therefore the particle size distribution became broader (Figure 2a). These results are in agreement with previous results reported when thiol-deficient conditions were used for the synthesis of Au nanoparticles [44]. The particles distribution becomes narrower whilst the amount of PVA was raised, thus leading to a narrower particle size distribution.

At lower concentration of Au ($5.08*10^{-4}$ M), a more defined picture was found, as illustrated in Table 1. Indeed, in this case increasing the amount of PVA, the average diameter decreases as already observed in previous experiments on Au_{PVA}/TiO_2 [42]. When the PVA/Au wt/wt ratio was adjusted to 0.3, the formation of large nanoparticles was observed (median particle size of 6.7 nm) along with a broader distribution of nanoparticle size (Figure S3). Increasing the PVA/Au wt/wt ratio from 0.3 to 0.65 and 1.2 resulted in a decrease of the mean particle size from 6.7 nm to 3.8 nm and 3.1 nm, respectively (Table 1). The peculiar behaviour using PVA/Au ratio to 2.0 is confirmed, leading to an increase of median particle size of 4.9 nm). These results demonstrate that there is an optimum ratio between PVA and Au for the formation of gold nanoparticles in the range of 3-4 nm.

In addition, at low or high PVA/Au ratio the synthesis of larger nanoparticles in the 5-6 nm range is feasible.

When these experiments were extended to even lower Au concentration ($1.69*10^{-4}$ M) the size of the gold nanoparticles was in the range of 3-4 nm when the PVA/Au wt/wt ratio was varied between 0.3-1.2. In fact, a progressive increase of the PVA/Au wt/wt ratio from 0.65 to 1.2 slightly decreased the median particle size from 3.91 to 3.5, whereas increase of PVA/Au wt/wt ratio from 0.3 to 0.65 did not affect the final particle size. Higher PVA/Au (PVA/Au = 2 wt/wt) produced (as demonstrated in the previous cases) larger nanoparticles, of 7.4 nm.

It is of interest to compare the effect of Au concentration at the same value of PVA/Au wt/wt ratio. Increasing gold concentration when the PVA/Au wt/wt ratio was maintained at 0.65 and 1.2, an increase of mean particle size was observed. The larger mean particle size was obtained with the highest concentration of Au (4.8 nm), followed by the lower concentrations of Au, where the gold nanoparticles produced did not differ (3.8-3.9) (Table 1). However, a more complicated picture was observed when the PVA/Au wt/wt ratio was at the lowest (0.3) and the highest value (2.0). In these cases, growth of gold nanoparticles was observed with more diluted Au solutions, however, this trend was not the same for both PVA/Au wt/wt ratio used.

The above results indicate that with Au concentration varied between $1*10^{-3}$ M to $1*10^{-4}$ M and PVA/Au wt/wt ratio of 0.65 and 1.2, gold supported nanoparticles in the range of 3-5 nm were synthesised with narrow particle size distribution. In fact, the smallest gold supported nanoparticles produced were with PVA/Au wt/wt ratio of 0.65 and 1.2 for the whole range of Au concentrations. With PVA/Au wt/wt ratio of 0.3 and 2.0 the mean particle sizes of the supported gold nanoparticles varied between 4 to 7 nm.

3.3. Effect of Au concentration and PVA/Au wt/wt ratio on the 1 wt% Au/TiO_2 samples

Analogous preparations were also undertaken with colloidal gold particles and depositing them onto titania. In these experiments, the preparation of gold nanoparticles was focussed on using Au concentrations of $1.02*10^{-3}$ M and $5.08*10^{-4}$ M and the PVA/Au ratio (wt/wt) was adjusted to 0.65, 1.2 and 2.0. Using $1.02*10^{-3}$ M of Au concentration (Table 1) the median particle size of the supported gold nanoparticles increased with subsequent increase of PVA/Au wt/wt ratio. In fact, the particle size increased from 4.0 nm to 6.3 nm and to 7.0 with increase of PVA/Au wt/wt ratio of 0.65 to 1.2 and 2, respectively (Table 1). The same trend was observed at lower concentration of Au ($5.08*10^{-4}$ M) with particle size that varied from 4.2 nm to 4.8 nm and to 5.0 with increase of PVA/Au wt/wt ratio of 0.65 to 1.2 and 2, respectively (Table 1).

These results showed that by the Au concentration has not a substantial effect on Au particle size when TiO_2 was used as support. On the contrary a decrease of Au particle size was obtained by using a large amount, as already evidenced for carbon supported nanoparticles.

3.4. Comparison between unsupported and supported Au colloids

For studying the effect of support on the particle size diameter of gold colloids before and after deposition on the support, TEM analysis was performed for one synthesised colloid with [Au] = $5.08*10^{-4}$ M and PVA/Au = 0.65 wt/wt ratio (Table 2).

TEM analysis was performed by placing a drop of the colloidal dispersion of PVA-Au nanoparticles onto a carbon-coated copper grid, followed by evaporating the solvent. TEM images (Figure 1) showed a very uniform distribution of gold nanoparticles that were spherical in shape. A histogram of the particle size distribution showed the presence of a very narrow particle size distribution with median particle size of 3.2 nm. Comparison with the Au supported colloids on carbon revealed that there was an increase of particle size from 3.2 nm to 3.8 nm for the colloid and the carbon supported, respectively. The presence of larger particles for Au/AC indicates the growth of nanoparticles during the immobilisation step, as it can be seen from the broader particle size distribution (Figure 1a and Figure S3C).

Comparison with the Au supported colloids on carbon and titania revealed that the growth of particle size during the deposition of the Au nanoparticles on the surface of carbon and titania was in a higher extent in the case of titania. The particle size increased from 3.2 nm to 4.2 nm for Au colloid and Au/TiO_2 titania, respectively (Table 2). This result clearly suggests that the surface of the support affects to some extent the particle size dimension and particle size distribution, by a moderate growth of particle size. The shape of the nanoparticles at this range of particle diameter is spherical, in agreement with the observation of previous reported data [40].

3.5. Effect of heat treatment process

The effect of heat-treatment was studied for a series of Au colloids supported on carbon and titania. Table 4 a summary of the median Au size TEM data are presented whereas selected TEM images and particles distribution are shown in Figures S7 and S8. In general, an increase of particle diameter and polydispersity of Au nanoparticles was observed after the calcination step. However, the degree of increase of particle size and standard deviation appears to be depended on the ratio of PVA/Au and type of support used for the deposition of the Au nanoparticles. By varying the PVA/Au ratio, using the same Au concentration, in the case of the 1 wt% Au/C samples, we observed a significant growth of particle size from 4.1 to a bimodal distribution centered in 7.7 and

17.9 nm with PVA/Au = 0.65, whereas with PVA/Au = 1.2 the growth was from 7.4 nm to a bimodal distribution centered in 7.5 and 12.4 (Table 4 and Figure S7). Note that the growth of particle is more evident with the lower PVA/Au ratio (0.65) showing that the amount of PVA used seems to affect significantly the growth process of the Au nanoparticles on the surface of the carbon.

In the case of the 1wt% Au/TiO_2 samples the calcination step appeared to less affect the final Au particle size. With a PVA/Au wt/wt ratio of 0.65 the TEM analysis revealed that the median particle size increased from 4.2 nm to 10.2 nm and with PVA/Au wt/wt ratio of 1.2, the increase of mean particle size was from 4.8 nm to 5.6 nm. These results strongly indicate that both PVA/Au ratio and the kind of support used influenced the growth process of Au nanoparticles during the calcination step. Presumably, the role of PVA as protecting layer around the gold nanoparticles is to act as an inhibitor agent during the heat treatment during the particle growth process. In addition, by using titania instead of carbon the degree of metal-support interaction is different and it seems that with titania is stronger, since the extent of particle size growth is lower with titania than carbon with the same PVA/Au wt/wt ratio. The effect of metal support interaction is illustrated by taking into account the Au $4f_{7/2}$ binding energies (BE) as determined by XPS. For Au/TiO_2 Au $4f_{7/2}$ BE showed a negative shift (83.1 eV, metallic gold has BE of 84.2 eV), which has been explained by electron transfer to the gold by the support and therefore suggesting strong metal-support interaction, whereas in the case of Au/C we have not observed this trend. Increase of calcination temperature to 250 °C had a negligible effect in terms of BE (Table S1).

3.6. Catalytic results

3.6.1. Liquid phase oxidation of glycerol

A series of the synthesised Au supported catalysts were tested in the liquid phase oxidation of glycerol for revealing the effect of PVA in terms of catalytic activity and selectivity. The liquid phase oxidation of glycerol was chosen as the model reaction for polyol oxidation due to the fact of its high reactivity and the existence of a complex reaction network [22]. This reaction is of specific interest because glycerol is a byproduct of biodiesel synthesis from triglyceride feedstocks [46]. During the biodiesel production, 10 wt% of the product corresponds to the formation of glycerol, implying that the glycerol market will experience a surplus [46].

Results are shown in Tables 3-4. In the case of using carbon as the supported material by increasing PVA/Au wt/wt ratio from 0.3 to 1.2 the activity (based on turnover frequency calculated on total numbers of surface atoms Ns) increased from 4609 to 4824 and to 10045 h^{-1}, for PVA/Au

ratio of 1.2, 0.65 and 0.3, respectively (Table 3). These results are in line with what observed in previous study, where Au catalysts with smaller amount of PVA show a better activity despite the bigger particles than in presence of a higher amount of protective agent [42]. A high amount of protective agent probably blocks the active site, thus decreasing the activity. Increasing the PVA/Au ratio from 1.2 to 2 an unexpected increase of activity was obtained (4609 and 9615 h^{-1}, for PVA/Au ratio 1.2 and 2, respectively), despite the larger amount of PVA and bigger particles of the catalyst with PVA/Au ratio of 2 (Table 3). It has been previously reported that the same anomalous trend was observed in the case of ethylene glycol oxidation using gold catalysts [47]. It has been reported that the activity did not follow the normal expected trend, but a maximum of activity has been observed in a range of 6–7 nm. The effect was correlated to the peculiar nature of active carbon that can shield the smallest particles. Indeed by decreasing the particle size the atomic percentage of Au with respect to C (at.% Au4f/C1s), measured by XPS, was found to decrease instead of increase due to the microstructure of the carbon material. These results confirmed that the activity is affected by a number of factors such as particles size, the amount of the protective agent and the microstructure of the support. Indeed the presence of a higher amount of PVA limited the access of the reactant to the active site decreasing the activity [40, 41]. Figure S9 reported the typical reaction profile observed for all the catalysts. The reaction profile for Au/TiO_2In terms of selectivity the major product was glyceric acid followed by glycolic and tartronic acids. Selectivity to glyceric acid was in the range 63-68%.

In the case of gold nanoparticles supported on titania, the catalytic activity was generally lower than that of the analogous Au/C samples (TOFs in the range 2771 – 4766 h^{-1}). A different trend was observed than AC supported Au. The activity did not significantly change from PVA/Au ratio of 1.2 and 0.65 (TOF of 2851 and 2771 h^{-1}, respectively), whereas the best results was obtained using an excess of PVA (PVA/Au= 2) (TOF of 4766 h^{-1}, respectively). All the catalyst showed a selectivity to glyceric acid higher (71-73%) than in the case of Au on carbon. This result is probably due to larger particles size in the case of Au on titania and a possible effect of the support on the degradation of glyceric to C-C cleavage cleavage.[33] It should be noted that the selectivity did not significantly changed at low and high conversions (Fig. S10, S11).

The structure sensitivity of the Au supported nanoparticles was investigated by relating the catalytic data produced from the effect of heat treatment to the Au particle size. The catalytic data is shown in Table 4. Calcination of the catalysts at 250 ºC under static air conditions led to a growth of the mean gold particle size, implying that the proportion of the high (terrace atoms) and low-coordination atoms (edge and corner) exist on the surface will alter with variation of particle size. It is expected that a higher number of high coordinated atoms will be formed as the particle size

increase [48]. The growth of particle size was influenced from the PVA/Au wt/wt ratio and the nature of the support, as discussed previously. By increasing the mean particle size the catalytic activity was substantially decreased by a factor of 2. These results indicate that the reaction is structure-sensitive. The existence of an optimum particle size implies that optimisation of the ratio of low-coordinated atoms to the high coordinated atoms is required for the conversion of glycerol.

In terms of selectivity, a different trend was observed between the carbon and titania supported gold nanoparticles. A slightly higher selectivity to glyceric acid was obtained in the case of carbon supported gold nanoparticles, whereas selectivity to glycolic acid remained almost unchanged. Selectivity to tartronic acid decreased as the gold particle size increased, indicating that the over-oxidation of glyceric acid to tartronic acid declined with increasing gold particle size, in agreement with previous results [49,50]. These results indicate that increasing the selectivity to glyceric acid requires the existence of larger Au nanoparticles, meaning that a higher proportion of high-coordinated atoms to low-coordinated atoms is an important requirement. Smaller Au nanoparticles are responsible for the over-oxidation of glyceric acid to tartronic acid. Therefore, the influence of gold particle size is also evident in the distribution of products; however, this is not to the same extent as observed in the catalytic activity. With gold nanoparticles supported on titania, the growth of gold particle size in the case of PVA/Au ratio of 0.65 resulted in a decreased activity (Table 4). On the contrary, for PVA/Au ratio of 1.2, the limited growth of Au size during calcination step resulted in a similar activity (Table 4).

4. Conclusions

A series of monometallic supported catalysts were synthesised by varying the PVA/Au wt/wt ratio and Au concentration and tested in the liquid phase oxidation of glycerol. Variation of PVA/Au wt/wt ratio and gold concentration influenced the gold particle size and particle size distribution obtaining gold supported catalysts in the range 3-7 nm. Moreover, the influence of support was evident.

In the case of carbon, the general trend in the influence on the size of the gold particles was that by increasing PVA/Au wt/wt ratio a progressive decrease in the mean gold particle diameter was occurred. However, at PVA/Au wt/wt ratio higher than 1.2 an increase in the mean gold diameter was found independently of the gold concentration. Regarding the effect of gold concentration, it was found that by increasing the gold concentration, the variation of the PVA/Au wt/wt ratio to the gold particle size was less significant.

In the case of titania supported gold catalysts, an increase in the PVA/Au wt/wt ratio led to a progressive increase in the mean gold particle diameter at high gold concentration. In contrast, the

variation of PVA/Au wt/wt ratio did not appreciably alter the mean gold diameter at lower gold concentration.

In terms of catalytic activity, high TOF was observed in all the cases and in the case of carbon supported catalysts the highest catalytic activity was found for the lower PVA/ratio. With titania supported catalysts, since similar mean gold particle diameter was found, the highest TOF was obtained with the narrowest particle size distribution, which was at PVA/Au wt/wt ratio of 2.

The effect of heat treatment on selected carbon and titania supported catalysts was evident in the mean gold particle diameter and as well as in the catalytic activity. We observed an increase of mean gold particle diameter by a factor of 2, which was dependent on the PVA/Au wt/wt ratio and the support. Increasing the PVA/Au wt/wt ratio led to a smaller growth of gold particle size, whereas with titania the growth rate of gold particles was lower, therefore providing gold particles with smaller mean particle size than the corresponding carbon supported catalysts. In terms of activity a significant lower catalytic activity was found with the calcined carbon and titania supported catalysts.

In conclusion, we have shown the importance of PVA/Au wt/wt ratio, gold concentration, heat treatment, and choice of support in the synthesis of supported gold-based catalysts with variable gold particle size and the influence in the catalytic activity and distribution of products in the liquid phase oxidation of glycerol under aerobic conditions. We expect that the methodologies used in the presented work for varying particle size and morphology will have a general applicability on a number of catalytic and biomedical applications where control of particle size, influence of capping agent and morphology of particle influences the performance of gold colloids.

Acknowledgements

This work formed of the EU AURICAT project (Contract HPRN-CT-2002-00174) and we are grateful for funding this research.

References

[1] G. Schocn, U. Simon, Colloid Polym. Sci. 273 (1995) 101-117.

[2] J.J. Storhoff, C.A. Mirkin, Chem. Rev. 99 (1999) 1849-1862.

[3] P.M. Tessier, O.D. Velev, A.T. Kalambur, J.F. Rabolt, A.M. Lenhoff, E.W. Kaler, J. Am. Chem. Soc. 122 (2000) 9554-9555.

[4] C.P. Collier, R.J. Saykally, J.J. Shiang, S.E. Henrichs, J.R. Heath, Science 277 (1997) 1978-1981.

[5] A.S.K. Hashmi, G.J. Hutchings, Angew. Chem. Int. Ed. 45 (2006) 7896-7936.

[6] T.K. Sau, A. Pal, T. Pal, J. Phys. Chem. B 105 (2001) 9266-9272.

[7] A.S.K. Hashmi, Gold Bull. 37 **(**2004) 51-65.

[8] G. J. Hutchings, Chem. Comm. (2008) 1148-1164.

[9] C.D. Pina, E. Falletta, L. Prati, M. Rossi, Chem. Soc. Rev. 37 (2008) 2077-2095.

[10] C.D. Pina, E. Falletta, Rossi, Chem. Soc. Rev. 41 (2012) 350-369.

[11] M. Haruta, T. Kobayashi, H. Sano, N. Yamada, Chem. Lett. 4 (1987) 405-408.

[12] M. Haruta, N. Yamada, T. Kobayashi, S. Iijima, J. Catal. 115 (1989) 301-309.

[13] F. Moreau, G.C. Bond, A.O. Taylor, Chem. Commun. (2004) 1642-1643.

[14] R. Zanella, S. Giorgio, C-H. Shin, C. R. Henry, C. Louis, J. Catal. 222 (2004) 357-367.

[15] F. Moreau, G.C. Bond, A.O. Taylor, J. Catal. 231 (2005) 105-114.

[16] M. Comotti, W-C Li, B. Spliethoff, F. Schüth, J. Am. Chem. Soc. 128 (2006) 917-924.

[17] G.J. Hutchings, J. Catal. 96 (1985) 292-295.

[18] M. Haruta, Catal. Today 36 (1997) 153-166.

[19] S. Biella, L. Prati, M. Rossi, J. Catal. 206 (2002) 242-247.

[20] L. Prati, M. Rossi, J. Catal. 176 (1998) 552-560.

[21] F. Porta, L. Prati, J. Catal. 224 (2004) 397-403.

[22] C.L. Bianchi, P. Canton, N. Dimitratos, F. Porta, L. Prati, Catal. Today 102-103 (2005) 203-212.

[23] S. Carretin, P. McMorn, P. Johnston, K. Griffin, G.J. Hutchings, Chem. Commun. (2002) 696-697.

[24] S. Carretin, P. McMorn, P. Johnston, K. Griffin, C.J. Kiely, G.J. Hutchings, Phys. Chem. Phys. 5 (2003) 1329-1336.

[25] D.I. Enache, J.K. Edwards, P. Landon, B. Solsona-Espriou, A.F. Carley, A.A. Herzing, M. Watanabe, C.J. Kiely, J.D.W. Knight, G.J. Hutchings, Science 311 (2006) 362-365.

[26] A.K. Sinha, S. Seelan, S. Tsubota, M. Haruta, Angew. Chem. Int. Ed. 43 (2004) 1546-1548.

[27] K. Mori, T. Hara, T. Mizugaki, K. Ebitani, K. Kaneda, J. Am. Chem. Soc. 126 (2004) 10657-10666.

[28] A. Abad, C. Almela, A. Corma, H. Garcia, Tetrahedron 62 (2006) 6666-6672.

[29] N. Dimitratos, A. Villa, D. Wang, F. Porta, D. Su, L. Prati, J. Catal. 244 (2006) 113-121.

[30] A. Biffis, S. Cunial, P. Spontoni, L. Prati, J. Catal. 251 (2007) 1-6.

[31] A. Villa, N. Janjic, P. Spontoni, D. Wang, D.S. Su, L. Prati, Applied Catal. A 364 (2009) 221-228.

[32] P. Haider, A. Baiker, J. Catal. 248 (2007) 175-187.

[33] A. Villa, N. Dimitratos, C. E. Chan-Thaw, C. Hammond, L. Prati, G. J. Hutchings, Acc. Chem. Res. 48 (2015) 1403−1412

[34] T. Ishikara, Y. Ohura, S. Yoshida, Y. Hata, H. Nishiguchi, Y. Takita, Appl. Catal. A: General 291 (2005) 215-221.

[35] C. Burato, P. Centomo, M. Rizzoli, A. Biffis, S. Campestrini, B. Corain, Adv. Synth. Catal. 348 (2006) 255-259.

[36] Y. Nomura, T. Ishihara, Y. Hata, K. Kitawaki, K. Kaneko, H. Matsumoto, ChemSusChem 1 (2008) 619-621.

[37] J. K. Edwards, G. J. Hutchings, Angew. Chem. Int. Ed. 47 (2008) 9192-9198.

[38] J.K. Edwards, E. Ntainjua, A.F. Carley, A.A. Herzing, C.J. Kiely, G.J. Hutchings, Angew. Chem. Int. Ed. 48 (2009) 8512-8515.

[39] J.K. Edwards, B. Solsona, E. Ntainjua, A.F. Carley, A.A. Herzing, C.J. Kiely, G.J. Hutchings, Science 323 (2009) 1037-1041.

[40] L. Prati, A. Villa, Acc. Chem. Res. 47 (2014) 855–863.

[41] J.A. Lopez-Sanchez, N. Dimitratos, C. Hammond, G.L. Brett, L. Kesavan, S. White, P. Miedziak, R. Tiruvalam, R.L. Jenkins, A.F. Carley, D. Knight, C.J. Kiely, G.J. Hutchings, Nat. Chem. 3 (2011) 551-556.

[42] A. Villa, D. Wang, G. M. Veith, F. Vindigni and L. Prati, Catal. Sci. Technol. 3 (2013) 3036-3041.

[43] N. Dimitratos, J. A. Lopez-Sanchez, D. Morgan, A. Carley, L. Prati, G. J. Hutchings, Catal. Today 122 (2007) 317-324.

[44] R. G. Shimmin, A.B. Schoch, P.V. Braun, Langmuir 20 (2004) 5613-5620.

[45] A. Corma, S. Iborra, A. Velty, Chem. Rev. 107 (2007) 2411-2502.

[46] J.J. Bozell, G.R. Petersen, Green Chem. 12 (2010) 539-554.

[47] F. Porta, L. Prati, M. Rossi, S. Coluccia, G. Martra, Catalysis Today 61 (2000) 165-172.

[48] J. Chen, Q. Zhang, Y. Wang, H. Wan, Adv. Synth. Catal. (350) 2008 453-464.

[49] N. Dimitratos, J.A. Lopez-Sanchez, D. Lennon, F. Porta, L. Prati, A. Villa, Catal. Letters 108 (2006) 147-153.

[50] W.C. Ketchie, Y-L. Fang, M.S. Wong, M. Murayama, R.J. Davis, J. Catal. 249 (2007) 328-337.

Figure Captions

Scheme 1. Reaction scheme for glycerol oxidation.

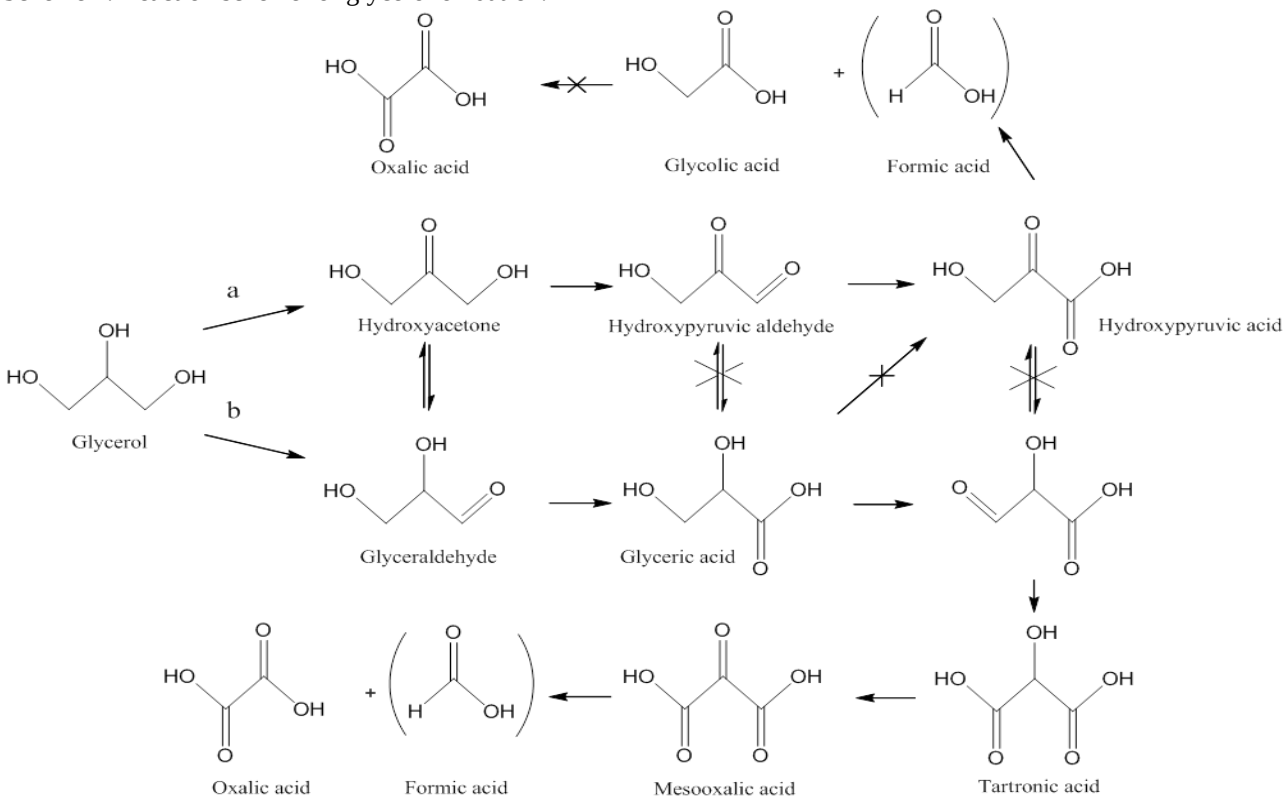

Fig. 1. TEM micrographs and distribution of gold colloidal particles, a) small scale-10 mg of Au, b) large scale -50 mg of Au, [Au]= $5.08*10^{-4}$ M, PVA/Au=0.65

a)

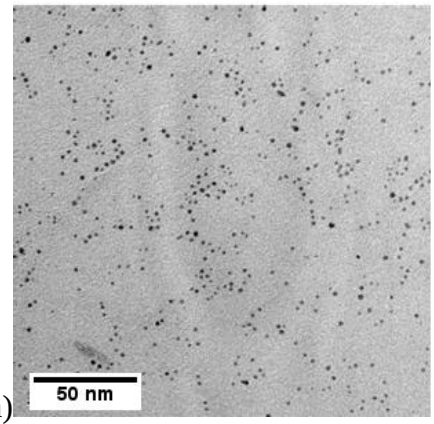

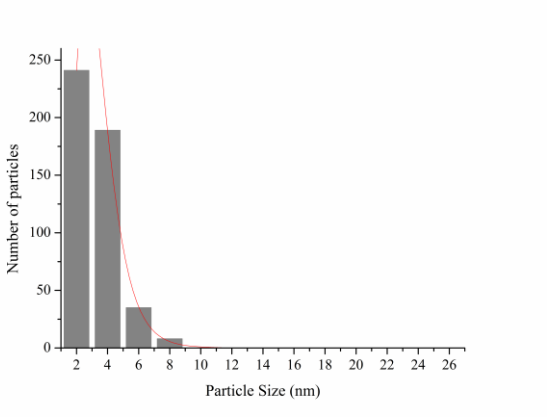

b)

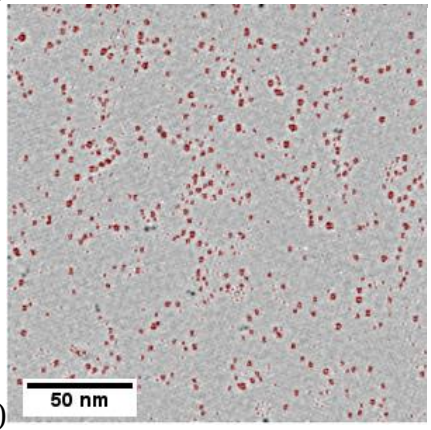

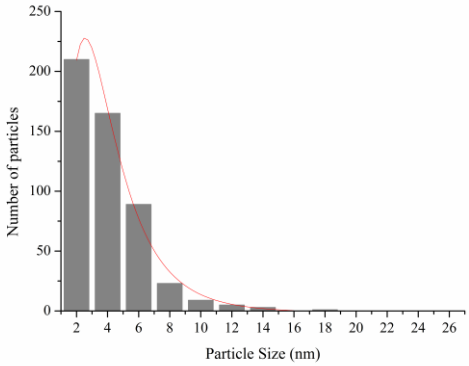

Fig. 2. TEM micrographs and distribution of gold colloidal particles ([Au]=1.02*10^{-3}) supported on carbon, a) PVA/Au=0.3, b) PVA/Au=0.65, c) PVA/Au=1.2, d) PVA/Au=2.0.

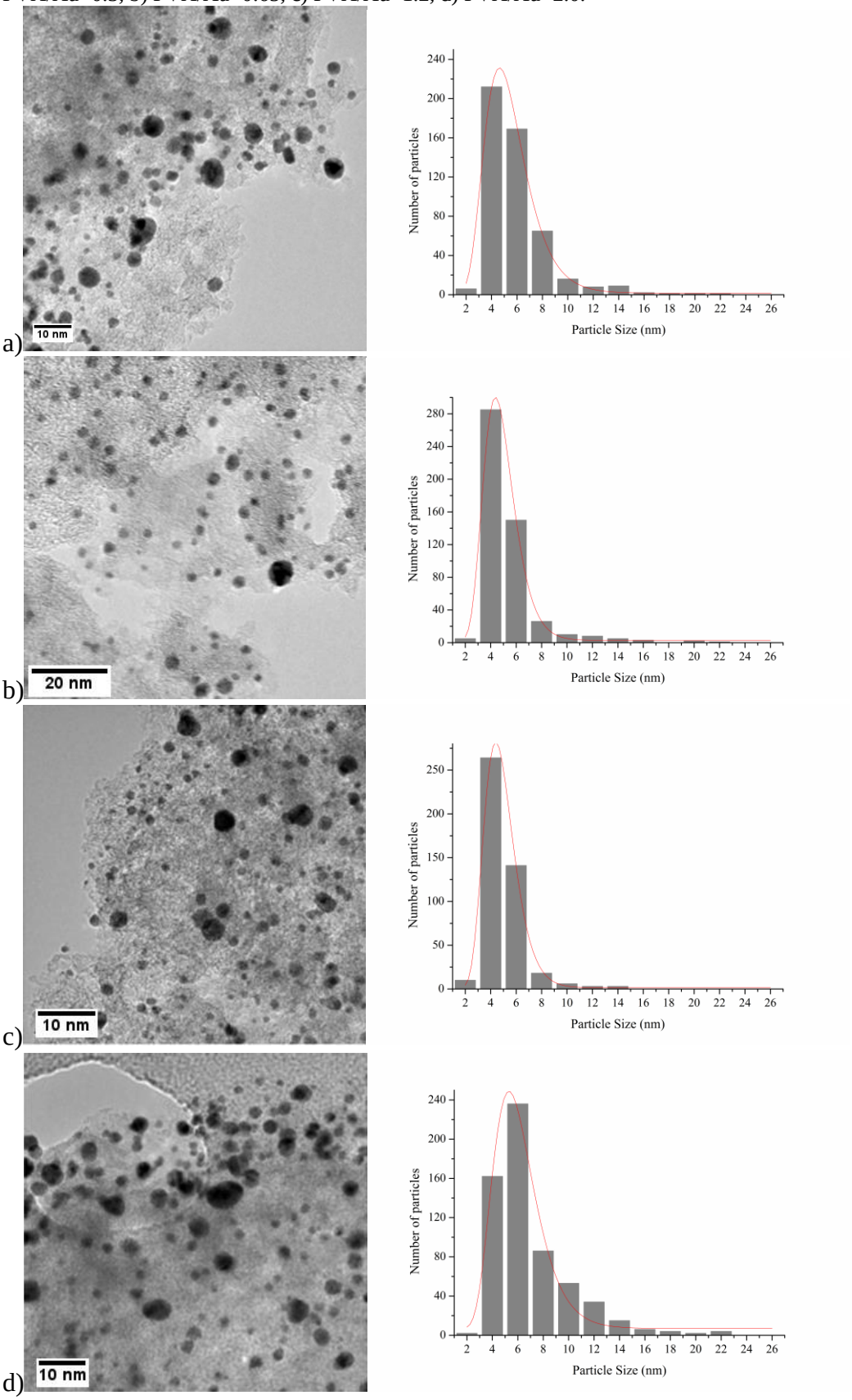

Tables

Table 1. Particle sizes for Au nanoparticles supported on TiO_2 and Carbon

[Metal] (mol L^{-1})	PVA/Au wt/wt (g)	*Median* (nm)
Supported on Carbon (GXS)		
$1.02*10^{-3}$	0.3	5.1
$1.02*10^{-3}$	0.65	4.8
$1.02*10^{-3}$	1.2	4.7
$1.02*10^{-3}$	2.0	5.8
$5.08*10^{-4}$	0.3	6.7
$5.08*10^{-4}$	0.65	3.8
$5.08*10^{-4}$	1.2	3.1
$5.08*10^{-4}$	2.0	4.9
$1.69*10^{-4}$	0.3	4.0
$1.69*10^{-4}$	0.65	3.9
$1.69*10^{-4}$	1.2	3.5
$1.69*10^{-4}$	2.0	7.4
Supported on TiO_2 (Anatase)		
$1.02*10^{-3}$	0.65	4.2
$1.02*10^{-3}$	1.2	6.3
$1.02*10^{-3}$	2.0	7.0
$5.08*10^{-4}$	0.65	4.0
$5.08*10^{-4}$	1.2	4.8
$5.08*10^{-4}$	2.0	5.0

Table 2. Particle sizes for unsupported gold nanoparticles and gold nanoparticles supported on TiO_2 and Carbon

Samples	[Metal] (mol L^{-1})	PVA/Au wt/wt (g)	*Median* (nm)
Colloid	$5.08*10^{-4}$	0.65	3.2
1%Au/C	$5.08*10^{-4}$	0.65	3.8
1%Au/TiO_2	$5.08*10^{-4}$	0.65	4.2

Table 3. Liquid phase oxidation of glycerol using Au nanoparticles supported on TiO_2 and Carbon[a]

[Metal] (mol L^{-1})	PVA/Au wt/wt (g)	*Median* (nm)	Conv. (%)	Selectivity (%)					
				GLYA	GLYCA	TARAC	OXALA	FOA	TOF (h^{-1})[b]
Supported on Carbon (GXS)									
$5.08*10^{-4}$	0.3	6.7	95.0	65.5	11.9	11.2	1.6	9.8	10045
$5.08*10^{-4}$	0.65	3.8	93.0	67.9	14.7	6.8	0.7	9.9	4824
$5.08*10^{-4}$	1.2	3.1	92.1	66.8	13.8	7.3	1.0	11.1	4609
$5.08*10^{-4}$	2.0	4.9	95.7	62.6	13.0	12.7	1.7	10.0	9615
Supported on TiO_2 (Anatase)									
$5.08*10^{-4}$	0.65	4.0	70.5	72.5	14.2	4.1	0.5	8.7	2771
$5.08*10^{-4}$	1.2	4.8	65.0	70.9	14.7	3.6	0.4	10.4	2851
$5.08*10^{-4}$	2.0	5.0	68.2	73.7	13.5	3.4	0.6	8.8	4766

[a]Reaction conditions: total volume 35 ml, 0.3M glycerol, m_{cat}=50 mg, NaOH/Glycerol ratio=4 (mol/mol), glycerol/metal= 4137, T=50 ºC, pO_2=3atm, Time of reaction=6 h, stirring rate=1500 rpm.
[b]Calculation of TOF (h^{-1}) based on total number of surface atoms (Ns) after 0.50 hour of reaction. TOF numbers were calculated on the basis of totalloading of metals.
* Calculation of TOF (h^{-1}) after 1 hour of reaction.

Table 4. Liquid phase oxidation of glycerol using supported Au catalysts (dried and calcined)[a]

Samples	[Metal] (mol L^{-1})	PVA/Au wt/wt (g)	*median* (nm)	Conv. (%)	Selectivity (%)					TOF (h^{-1})[b]
					GLYA	GLYCA	TARAC	OXALA	FOA	
Supported on Carbon (GXS)										
Dried	$1.69*10^{-4}$	0.65	3.9	95.1	67.1	14.2	8.4	1.3	9.1	3988
Calcined	$1.69*10^{-4}$	0.65	7.7, 17.9[b]	79.3	73.0	13.3	4.4	0.4	9.0	1852
Dried	$1.69*10^{-4}$	2.0	7.4	91.6	70.9	13.5	5.9	0.5	9.2	5415
Calcined	$1.69*10^{-4}$	2.0	7.5, 12.4[b]	56.7	71.5	13.2	3.7	2.4	9.2	2514
Supported on TiO_2 (Anatase)										
Dried	$5.08*10^{-4}$	0.65	4.0	70.5	72.5	14.2	4.1	0.5	8.7	2271
Calcined	$5.08*10^{-4}$	0.65	10.2	54.9	66.1	17.9	4.2	0.8	11.0	873
Dried	$5.08*10^{-4}$	1.2	4.8	65.0	70.9	14.7	3.6	0.4	10.4	5953
Calcined	$5.08*10^{-4}$	1.2	5.6	31.9	64.9	16.7	4.6	0.4	13.3	5623

[a]Reaction conditions: total volume 35 ml, 0.3M glycerol, m_{cat}=50 mg, NaOH/Glycerol ratio=4 (mol/mol), glycerol/metal= 4137,T=50 ºC, pO_2=3atm, Time of reaction=6 h, stirring rate=1500 rpm.
[b]Calculation of TOF (h^{-1}) based on total number of surface atoms (Ns) after 0.50 hour of reaction. TOF numbers were calculated on the basis of total loading of metals.
c) Bimodal distribution